Preparation and Characterization of Synthetic Polypeptide Single Crystals with Controlled Thickness

Honggang Cui,[†] Vahik Krikorian,[†] Jeffery Thompson,[§] Andrew P. Nowak,[‡] Timothy J. Deming,[‡] and Darrin J. Pochan*[,†]

Department of Materials Science and Engineering and Delaware Biotechnology Institute, University of Delaware, Newark, Delaware 19716; Department of Bioengineering, University of California at Los Angeles, Los Angeles, California 90095; and Department of Materials and Chemistry, University of California at Santa Barbara, Santa Barbara, California 93106

Received April 12, 2005; Revised Manuscript Received June 13, 2005

ABSTRACT: Molecular crystallization provides an experimentally simple way to arrange molecules on the nanoscale. Synthetic polypeptides present the potential to control ultimate crystal structure by design of primary structure and/or secondary structure adjustment in solution during crystallization. In this work, hexagonal single crystals of synthetic poly-L-lysine (PLL) were produced from aqueous solution by the addition of divalent counterions. It was found that PLL having 100−200 amino acids crystallized in an unfolded-chain form with the crystal thickness controlled directly by PLL molecular weight. PLL chains exhibited chain folding in the crystal state when the PLL was greater than 265 residues. PLL with less than 100 residues were not crystallizable under the same crystal growth conditions. X-ray diffraction data revealed that PLL chains had an α-helical secondary structure and hexagonal symmetry in the crystal state. The introduction of divalent counterions is necessary to initiate the crystallization process and stabilize the crystal structure.

Introduction

Molecules can self-assemble into well-defined structures via nonconvalent interactions that provide a "bottom-up" approach to the fabrication of materials. Recently, molecular self-assembly has been widely used to obtain functionalized materials on the nanometer scale.[1−4] One of the simplest ways to produce a regular arrangement of molecular units is to grow a periodic crystal in two or three dimensions.[1] The first identification of polymer single crystals is attributed to three independent reports in 1957.[5−7] Since then, most traditional crystallizable polymers have been crystallized into single crystals by cooling a dilute solution from an elevated temperature or by adding nonsolvent to the polymer dilute solution.[8] Enormous effort has been devoted to elucidating the relations between macromolecular structure and supramolecular crystallization in order to control the final crystallized structure for specific applications. Polymer single-crystal structure involves four key parameters: chain conformation, unit cell structure, lamellae thickness, and surface structure.[9,10] Unfortunately, although traditional polymers crystallize from solution in regular lamellar forms with periodic chain folding and specific thickness, the four parameters mentioned above are hard to precisely control with traditional synthetic polymer building blocks or solution conditions in which polymer crystals grow. Studies on the crystallization of low molecular weight PEO fractions[11−14] and monodisperse *n*-alkanes[15,16] have shown that integral folding (IF) could offer potential ability to control lamellae thickness by varying molecular weight and supercooling temperature (isothermal thickening or thinning). However, this thickness control is limited to a small scale, and most of these crystals obtained, either from solution or melts, are a mixture of different fold numbers. Large, isolated single crystals with complete unfolded chains are difficult to obtain and normally require annealing at low surpercooling for a significant time.

Biomacromolecules, such as DNA and proteins, provide an opportunity for precise control over the abovementioned parameters due to their specific intra- and intermolecular hydrogen-bonding interactions. Examples in the literature that exploit the specificity presented by biomolecules include Seeman and coworkers,[1] who reported two-dimensional self-assembled crystals from synthetic DNA and used them as templates for making a periodic nanoscale pattern. Krejchi et al.[9] designed repeating polypeptides sequence of [(Ala-Gly)xGluGly] in which Ala-Gly dyads were selected to assemble into β-sheet crystal "stems" in lamellar aggregates with a controlled turn at the glutamic acid position. With this design, the thickness of the polypeptide crystals was specifically controlled by altering the number of dyads. In the work presented here, we take advantage of the controllable secondary structure of synthetic polypeptides and report the self-assembly of poly-L-lysine homopolypeptide (PLL) into single crystals of controlled thickness and symmetry. The crystal thickness is exactly controlled by the molecular weight and α-helical secondary structures of the PLL molecules. In addition, the crystal surface carries a periodic distribution of primary amine functionality matching the symmetry and spacing of the underlying crystals.

Although the crystallization behavior of conventional polymers is well developed, relatively few studies have addressed the crystallization behavior of synthetic polypeptides from aqueous solutions. Using traditional techniques for the growth of polymer single crystals from dilute solution, Padden, Keith, and their coworkers successfully prepared single crystals of poly-L-tyrosine,[17] poly-L-alanine,[17] poly-L-glycine,[17] poly-L-

[†] University of Delaware.
[‡] University of California at Los Angeles.
[§] University of California at Santa Barbara.
* Corresponding author. E-mail: Pochan@udel.edu.

10.1021/ma050776q CCC: $30.25
Published on Web 07/30/2005

lysine,[18] and poly(L-glutamic acid)[19,20] homopolypeptides, from aqueous solutions in the 1960s. In addition, Lotz and co-workers[21,22] studied the crystallization behavior of polyglycine I. To the best of our knowledge, these have thus far been the only successful reports of the single crystal formation of homopolypeptides. Similarly, Aldries et al.[23] crystallized poly(*O*-acetylhydroxy-L-proline), a derivative of poly-L-proline, and obtained the electron diffraction pattern of the single crystals. Single crystals of derivatives of poly(L-glutamic acid)[24] and poly(γ-methyl D-glutamate)[25] have also been produced. Most of the aforementioned homopolypeptides and their derivatives formed hexagonally shaped lamellar structures with α-helical chain conformations. β-Sheet crystals[18,20,26,27] can also be formed depending on growth conditions. Thus far in the literature, all the polypeptide single crystals are reported to have a folded-chain structure based upon the discrepancy of calculated extended molecular lengths with measured crystal lamellae thickness. By epitaxial crystallization on alkali halide single crystals, Rybnikar and Geil[28] reported that single crystals of poly(γ-benzyl L-glutamate) were composed of straight, nonfolded α-helical chains aligned side by side. Conversely, using the same method, Carr et al.[29] proposed that the epitaxial structure consisted of folded α-helical lamellae, based on electron diffraction. During the same time, some attention was paid to the crystallization behavior of copolypeptides.[30−33] However, unfolded solution-grown crystals of polypeptides have not yet been reported.

In this paper, we present the preparation and characterization of single crystals of narrow molecular weight distribution PLL by adding divalent counterions. Poly-L-lysine with 100−200 amino acid monomers crystallized without chain folding, which has not been reported previously. Because of the periodic distribution of primary amine functionality on the surface, these large, single-crystal platelets may provide a potential nanoscale to mesoscale template for the controllable arrangement of nanoparticles or biomineralization of inorganic salts. We also hope that familiarity with crystallization of synthetic polypeptides will give a better understanding of the crystallization behavior in more complex systems such as linear proteins with charged amino acids. In addition, this work may help to elucidate the chain length dependence of chain-folded crystallization in parallel systems such as low molecular weight poly(ethylene oxide) and *n*-alkanes which have been extensively studied with the aim of understanding chain-folding nature in polymer crystals.[16]

Experimental Section

Polymer Synthesis. All the poly-L-lysine samples were synthesized using a cobalt-initiated polymerization of α-amino acid-*N*-carboxyanhydrides (NCAs) as previously reported.[34,35] After the polymerization of the NCA, CBZ groups on the lysine side chains were removed with 33% HBr/HOAc aqueous solution. The polymers were washed several times and dialyzed against water to remove residue HBr. The chemical structure of PLL used in this study is shown in Figure 1. Table 1 shows all the poly-L-lysine samples used in this study. In this paper, PLL is represented by its single letter amino acid notation, K, followed by the number of residues. K_L indicates a polymer that has left-handed chirality, K_D shows right-handed chirality, and K_{rac} is the racemic random copolymer mixture of both chiralities.

Single-Crystal Growth. Poly-L-lysine was dissolved in deionized water and left for 4 h to ensure complete dissolution. 1 mL of 0.2 M ammonium monohydrogen phosphate (AMHP) was slowly added to 5 mL of 0.02 wt % PLL solution at room temperature. Precipitation of single crystals could be observed after 1 day.

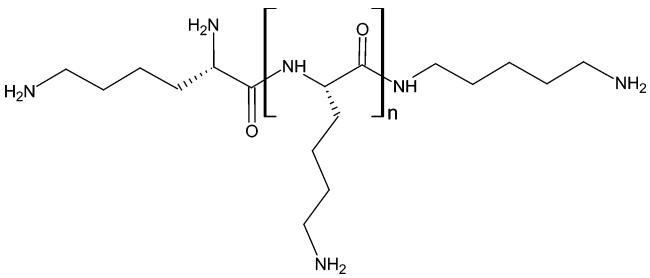

Figure 1. Chemical structure of poly-L-lysine used in this study.

Table 1. Molecular Characteristics of Polylysine Samples and Measured Single Crystal Thickness

polymers	PDI[a]	single crystals?	projected thickness (nm) (α-helical secondary structure)	measured thickness[b] by AFM (nm)	chain folding
K_L50	1.2	no			
K_L65	1.2	no			
K_L75	1.2	no			
K_L85	1.2	no			
K_L100	1.22	yes	15	14 ± 2	no
K_L115	1.15	yes	17.25	17 ± 2	no
K_L200	1.2	yes	30	24 ± 3	no
K_L265	1.23	yes	39.75	17 ± 2	yes
K_L310	1.15	yes	46.5	16 ± 2	yes
K_L550	1.2	yes	78	18 ± 2	yes
K_L1300	1.28	yes	195	18 ± 2	yes
K_{Rac}175	1.11	no			
K_{Rac}242	1.2	no			
K_D220	1.22	yes	33	20 ± 2	no

[a] Molecular weight (M_n) and polydispersity (M_w/M_n) were determined by tandem GPC/light scattering in 0.1 M LiBr in DMF at 60 °C using d*n*/d*c* values (c = concentration) measured in this solvent at λ = 633 nm.[35] [b] Thickness and deviation were determined from 50 different single crystals.

Electron Microscopy. Transmission electron microscopy (TEM) was performed on a JEOL JEM-2000FX TEM operating at an accelerating voltage of 200 kV. For the observation of morphology of PLL single crystals, 20−25 μL of dilute crystal suspension was dropped onto a copper grid coated with carbon film. After 2 min, excess solution was wicked away with filter paper, and the grid was allowed to dry in ambient conditions. Scanning electron microscopy (SEM) was performed on a JEOL JSM-7400F field emitting SEM. The instrument was operated at an accelerating voltage of 1 kV to minimize beam damage and to avoid negative charge buildup on the surface. A drop of solution was placed directly onto a plasma-cleaned silicon wafer and dried in ambient conditions.

Atomic Force Microscopy. Tapping mode atomic force microscopy was performed on a Multimode SPM equipped with a J scanner (Digital Instruments). The dilute crystalline suspensions were deposited onto freshly cleaned mica that was glued to a stainless steel sample disk. These samples were imaged using rotated monolithic silicon probes with aluminum reflex coating (BS-Tap300Al, Budget Sensors). The average height was given by at least 50 measurements from different sample areas.

Wide-Angle X-ray Scattering. Wide-angle X-ray scattering (WAXS) experiments were performed at the National Synchrotron Light Source at Brookhaven National Laboratory on the X10A beamline. The X-ray beam was monochromated with a double bounce germanium monochromator (λ = 1.566 Å). The concentrated crystal suspensions extracted from original dilute solution were transferred to boron-rich capillary tubes (Charles Supper Co.) with a 2.0 mm diameter. The detector, a Bruker CCD camera, was set at a distance of ~7 cm, and diffraction patterns were collected for 2 min.

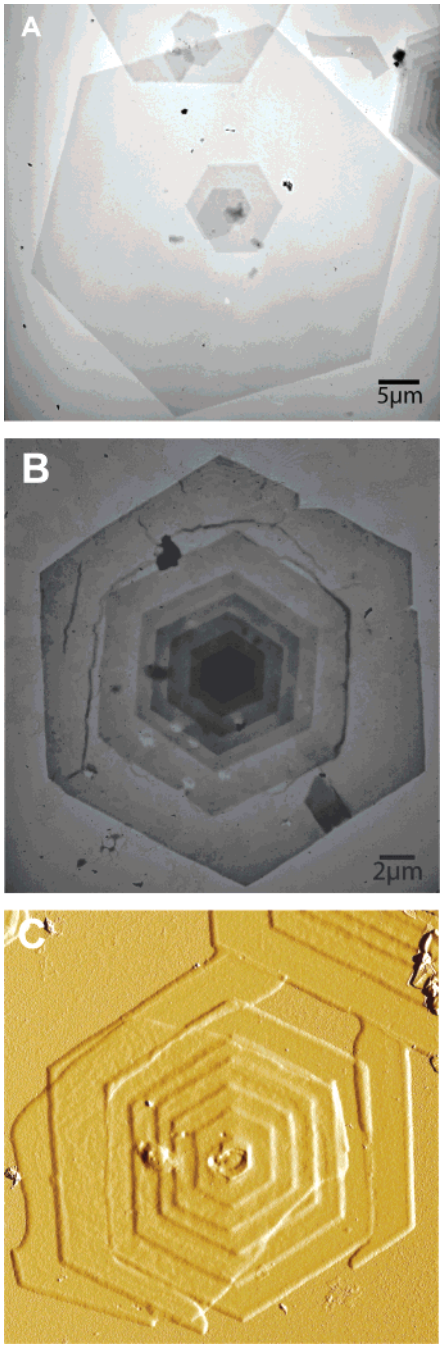

Figure 2. (A, B) TEM bright field images of K_L200 single crystals. (C) AFM amplitude image of K_L200 single crystal, 16 × 16 μm. All three images show hexagonally shaped single crystals.

Results and Discussion

Morphology and Structure. The regular morphology of single crystals was observed by direct deposition of the crystal suspension onto the carbon-coated copper grids. Figure 2 shows representative TEM images (Figure 2A,B) and a typical AFM image (Figure 2C) of PLL single crystals. Hexagonal crystals were formed with all PLL samples having more than 100 amino acid residues. Higher molecular weight PLL exhibited both monolamellar and multilamellar (with a central screw dislocation) single crystal forms, whereas lower molecular weight PLL samples had only monolamellar single crystals. PLL single crystals ranged in platelet size from a few to dozens of micrometers to some single crystals growing laterally out to 50 μm. Under the same growth conditions, lower molecular weight PLL always had smaller sized crystals based on TEM and AFM observations.

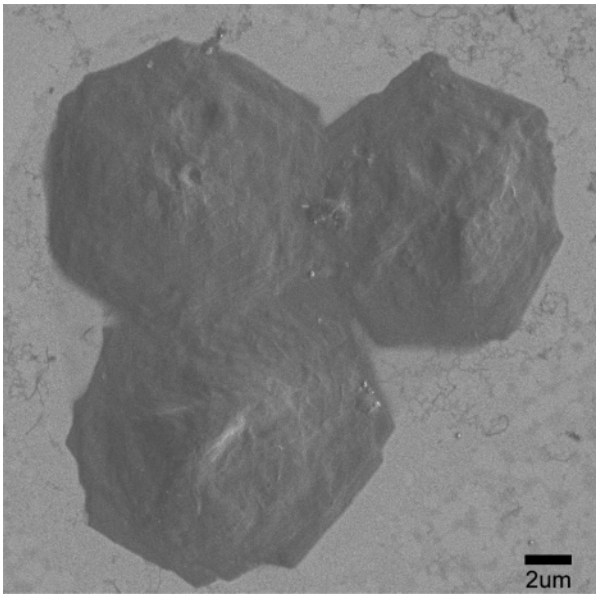

Figure 3. FESEM image of K_L200. The rough surface indicates the collapsed inner crystal structure after the complete removal of water.

Unlike traditional polymer single crystal growth methods from solution such as progressively cooling solution temperature or keeping solution at a constant supercooling (isothermal crystallization) or adding polymer nonsolvents, crystallization of PLL was performed by the addition of salts to aqueous solutions. In DI water, PLL chains are highly solubilized. Upon the addition of divalent salt, PLL chains crystallized in the form of α-helices. PLL single crystals are actually in the forms of PLL/AMHP complex because AMHP also takes part in crystals after crystallization. Divalent monohydrogen phosphate counterions can interact with two amine groups from adjacent helices and form a salt bridge. It is reasonable to assume that some water will remain in the interstices of the helices and interact with PLL chains due to the high affinity of PLL amine groups to water and the large spacing between helices (about 2 nm from XRD measurement, vide infra). In fact, the amount of water can play a significant role in helping stabilize polypeptide crystal structure.[36,37] Complete removal of water caused the collapse of the crystals. The collapsed crystals resulting from the drying process can be directly imaged using low-voltage field emitting scanning electron microscopy (Figure 3). The rough surface reflects the polypeptide collapse within the crystal structure.

Crystal diffraction was obtained by X-ray scattering from a single crystal suspension because we were not able to obtain electron diffraction pattern due to the collapse of crystal structure because of the complete removal of water for TEM samples. After crystallization, the crystals settled from suspension, requiring the X-ray beam to be carefully aligned through the bottom of the capillary tube. As shown in Figure 4A, the relatively diffuse weak peak at 5.4 Å is a characteristic feature of α-helices in peptides. Three reflections were also observed (shown in Figure 4B) that had values of $\sin^2\theta$ (where θ is the Bragg angle) with a ratio of 1:3:4. This ratio indicates that these are the first three ($hk0$)

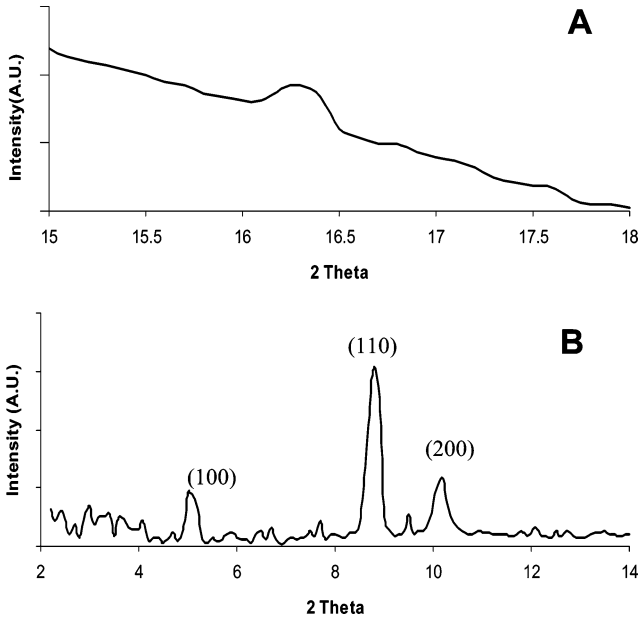

Figure 4. Integrated intensity vs 2θ from 2-dimensional WAXS measurement for K_L200 single-crystal suspension. (A) Characteristic α-helical peak at 5.4 Å. (B) Interhelix diffraction at low scattering angle; (100), (110), and (200) reflections had values of $\sin^2\theta$ (where θ is the Bragg angle) corresponding to a ratio of 1:3:4, indicating hexagonal symmetry. The peaks correspond to d spacings of 17.42, 10.10, and 8.72 Å, respectively. Both (A) and (B) were integrated from the same two-dimensional spectrum.

reflections from a hexagonal unit cell. The model of the crystal structure, based on scattering data, is shown in Figure 5A,B. PLL chains exhibited an α-helical conformation and packed in a hexagonal lattice. According to XRD data, the distance between two neighboring PLL helices is 20.20 Å. The fully extended side chain length of lysine (the distance from α-carbon to terminal nitrogen) has been reported as 5.5 Å.[38] The P−O bond length is ∼1.63 Å, and the NH−O hydrogen bonding length is ∼3.04 Å. Hence, the value for the extended lysine side chain double length between helices is calculated to be approximately 20.3 Å (Figure 5C). This calculated value matches very well with the XRD data and proves that the lysine side chains must be fully extended to interact with salt and side chains from their neighbor helices in order to stabilize the crystal structure. The phosphorus observed with X-ray energy dispersive spectroscopy operating within the SEM unambiguously revealed the presence of AMHP throughout the crystals thus supporting the lysine salt bridging mechanism (data not shown).

Thickness Controlled by Molecular Weight. Figure 6 shows AFM height images of PLL single crystals. The thickness of K200 single crystal lamellae is ∼26 nm (Figure 6C), which is reasonably close to the 30 nm length calculated for fully extended α-helices of K200 (1.5 Å per residue × 200 residues). Provided the molecular chain axes are oriented normal to the planes of the platelets in the single crystal state,[18] it can be concluded that the PLL chains are not folded. In an attempt to control crystal thickness, single crystals from

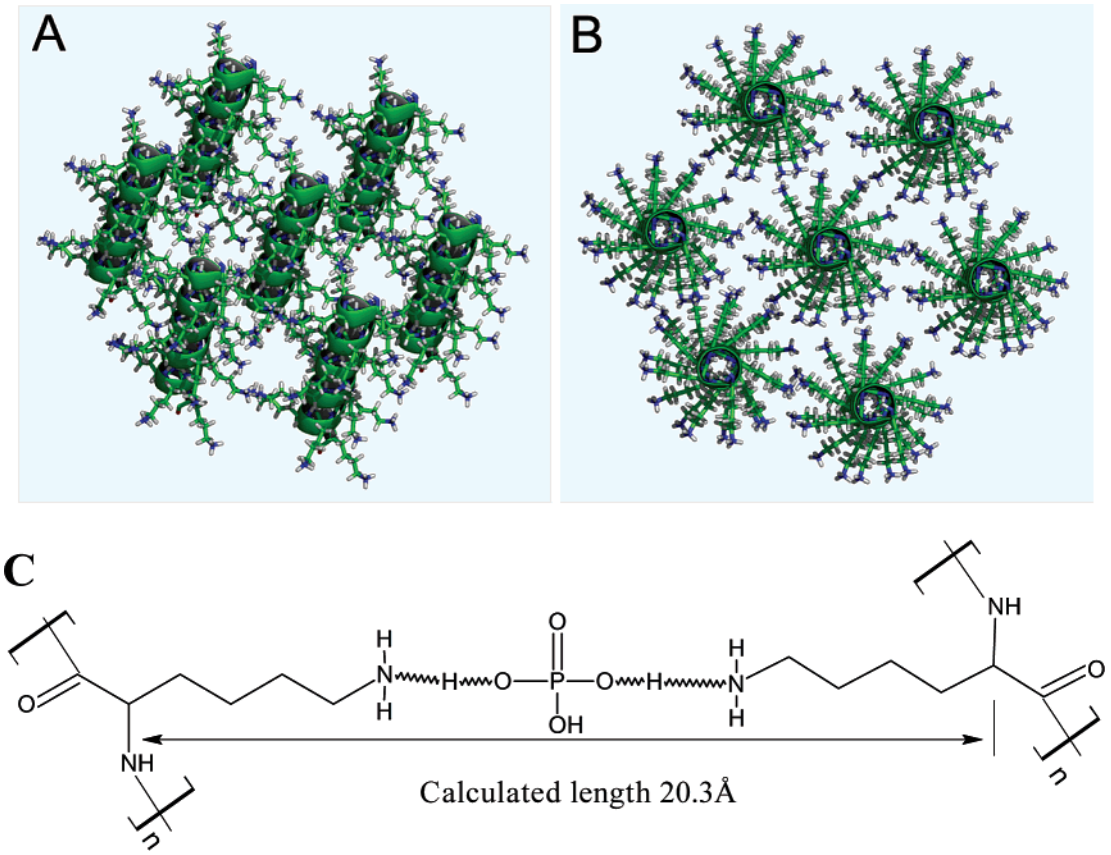

Figure 5. Schematic of PLL single-crystal structure having 100−200 residues: (A) side view; (B) top view of hexagonal packing of PLL α-helical chains. All the helices pack together without chain-folding. The conformation of PLL side chains is shown for clarity and does not imply a specific side chain structure in the crystal state. The AHMP counterions and water are not shown but would remain in the interstices between helices and interact with side chains to stabilize crystal structure. (C) Fully stretched lysine side chains and their interaction with divalent monohydrogen phosphate. Calculated length between two helices is around 20.32 Å, which matches very well with XRD measured distance 20.20 Å.

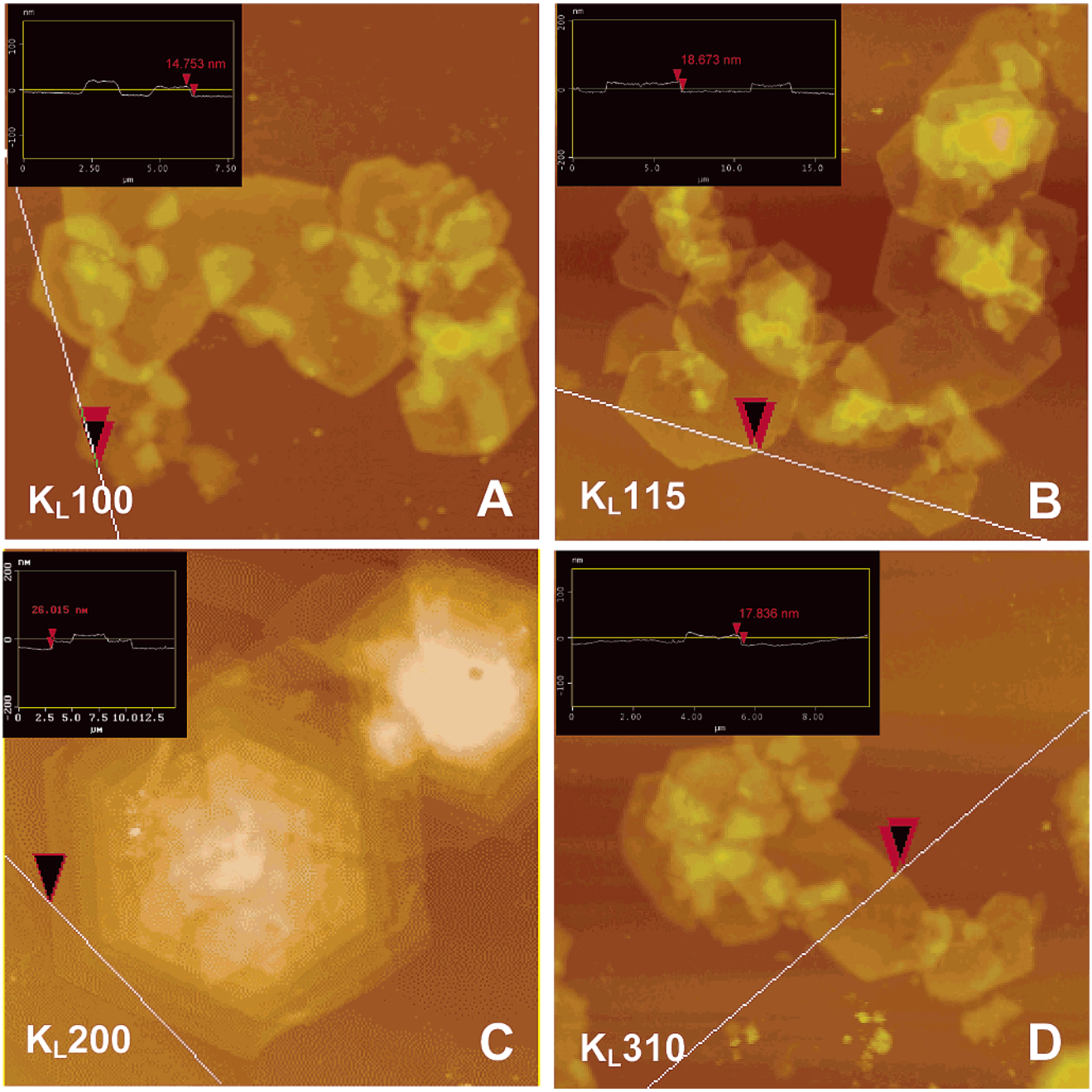

Figure 6. Representative AFM height images of (A) K_L100, (B) K_L115, (C) K_L200, and (D) K_L310; the image dimensions are 10 × 10, 17 × 17, 25 × 25, and 9 × 9 μm, respectively.

shorter PLL homopolymers (Table 1) were studied. As shown in Table 1, K100 and K115 also do not fold in the single crystal state exhibiting crystal thicknesses of ~14 and ~17 nm, respectively. Those thicknesses correspond to their theoretical α-helical chain length. Because of the metal-catalyzed living polymerization technique,[34] the studied polypeptides have a well-defined chain length (low PDI) and are stereoisomerically pure, thus enabling the ultimate precise control of crystal thickness from the molecular level. Therefore, the thickness of the single crystals can be controlled by adjusting the molecular weight of the homopolypeptide.

Studies with higher molecular weight showed PLL chain folding when the polymer had equal to or greater than 265 residues. The measured crystal thickness of K265 is ~17 nm, which is half of the fully extended α-helical chain length. K310 single crystals have a measured thickness of ~16 nm, which is one-third of its fully extended chain length. All higher molecular weight PLL exhibited chain folding in the crystals with a thickness of 18 nm, as shown in Table 1. This folding phenomenon of high molecular weight PLL is consistent with a previous report[18] in which two PLL samples with the estimated molecular weight of 90 000 and 150 000 Da (around 440 and 730 residues, respectively) crystallized in a hexagonal form with folded chains. A plot of thickness vs degree of polymerization of poly-L-lysine is shown in Figure 7.

It is generally believed that folded-chain architecture is a kinetic trap for crystallized, flexible polymer chains. Since chain-folded polymer crystals are metastable, they tend to thicken when annealing at elevated temperature. Spegt[11] reported crystals of low molecular weight PEO fractions lamellar thickness in a stepwise manner based on SAXS studies. Each step corresponded to one integer folded form. Soon thereafter, Kovacs et al.[39]

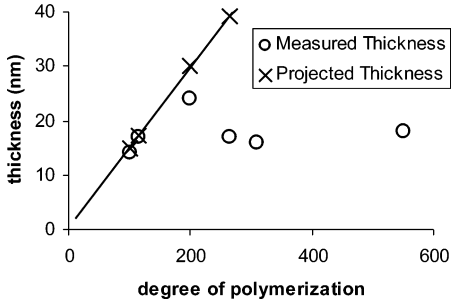

Figure 7. Plot of thickness vs degree of polymerization of poly-L-lysine. The thickness was measured by AFM. PLL with 100−200 residues have unfolded-chain single crystal forms as determined from the comparison of AFM measured vs projected thickness. PLL chains start folding with the residues greater than 265.

systemically reported that single lamellar crystals grown from low molecular weight PEO fractions and their isothermal thickening behavior. Unfolded and once-folded crystals can be obtained in PEO depending on molecular weight and supercooling temperature. Integral folding in PEO fractions may be due to the specific nature of the OH end groups and their hydrogen-bonding tendency.[16] The unfolded-chain structure in shorter PLL single crystals can be attributed to the rigid property of α-helical chains, strong interaction between extended side chains, and large spacing among helices. First, because of intramolecular hydrogen bonding between neighboring turns of the helix, the α-helical PLL chains are rigid. It is reasonable to assume that it is unfavorable for the α-helical chains to fold, and they would, therefore, retain their straight helical structure. Second, α-helical PLL chains stabilize the crystal structure mainly via hydrogen bonding and ionic interactions of the side chains. Besides the expense of losing intrachain hydrogen bonding, chain folding also causes more disruption of side chain interactions, resulting in an energy penalty. Third, the large spacing between helices provides for helix mobility during crystallization. Extended chain crystals have been observed in conventional polymers when polymer melts were cooled under pressure.[40−43] It was predicted that pressure crystallization would produce polymers in a mobile phase that prefer to form extended chain crystals and polymers in a more ordered and less mobile phase that form folded chain crystals.[42,44−46] The hexagonal phase is referred to as "mobile phase"[44] because the chains are loosely packed.[42,43] Unfolded PLL single crystals may fit into this category of mobile, hexagonal phase. Helices are hexagonally packed in the PLL crystal state, and the distance between two adjacent helices is ∼2 nm. The PLL helices may have relatively high mobility during crystallization that produces predominantly unfolded chain packing in samples with less than 200 residues.

Single crystals were not obtained from PLL chains with less than 100 residues. The unsuccessful preparation of single crystals from the lower molecular weight PLL can be attributed to unstable nucleus formation due to the small number of residues that prevented further chain association. In dilute PLL solution, the molecular nucleation for shorter PLL is not kinetically possible. When PLL has a residue number higher than 200, the ratio of molecule length to radius increases and the helix becomes relatively more flexible. It is more likely that the folded chain structure could be kinetically trapped. Long PLL also gains more chances to have conformational defects and fold within the crystal. It should be noted here all the single-crystal preparations were carried out under the same solution conditions. With growth condition changes, i.e., at higher temperature, the folded PLL single crystals of high molecular weight may form unfolded single crystals. It also cannot be excluded that the uncrystallized low molecular weight PLL may have other crystallized forms, like β fibrils, or crystallize under other solution conditions, such as lower temperature and high pH or by using salts and nonsolvents simultaneously. The influence of solution conditions on crystal morphology is currently under investigation.

Crystallization of Poly-L-lysine and Poly-D-lysine. Although pure solutions of poly-D-lysine (PDL) crystallize similarly to PLL, random racemic copolymers of D-lysine and L-lysine do not form single crystals. Crystallization of both $K_{rac}175$ and $K_{rac}242$ was attempted under the same crystal growth conditions as the enantiomerically pure K_L polymers. K_{rac} solutions remained optically clear for months after counterion addition with no crystals observable in TEM. Racemic polylysine may not form α-helices because the random distribution of L-lysine and D-lysine residues along the backbone disrupts the intrachain hydrogen bonding, preventing further crystallization. Fuhrhop et al. [47]obtained a β-sheet precipitate by mixing two aqueous solutions of helical PDL and PLL at pH 11 at room temperature. To reproduce their results, the pH of separate solutions of PDL (220 residues) and PLL (200 residues) were adjusted to 11 by adding ammonia. Both polymers exhibited an α-helical conformation according to circular dichroism spectra. Upon mixing, crystallization did not occur over a period of several months. Differences in these results from Fuhrhop et al. may arise from the different buffer solutions used to adjust solution pH since the salts in the buffer can influence the polymer secondary structure before crystallization. With the addition of AMHP counterions, the mixed solution of K_D220 and K_L200 produced hexagonal single crystals at room temperature within several days.

Conclusions

Single crystals of PLL with unfolded chains were produced by the addition of divalent salts to aqueous polymer solution. The thickness of the lamellar crystals was controlled by molecular weight. The single crystals exhibited chain folding above 265 residues. It was also found that PLL samples with less than 100 residues were unable to form crystals. PLL chains exhibited α-helical conformations and packed in a hexagonal lattice.

The unfolded hexagonal single crystals may prove useful for the development of nanoscale hybrid materials due to the periodic display of the chain termini on the crystal surfaces. The PLL polymers studied here have identical chain ends as a result of the synthesis, thus making both PLL crystal surfaces chemically the same. The net surface charge can be tuned by solution pH because of the weak basic nature of amine groups, and the positively charged surfaces can be converted to negative surfaces by the introduction of divalent or trivalent anions. The crystal surfaces may be used as templates to arrange nanoparticles with opposite charges. Surface functionality can also act as a highly ordered growth center to direct the mineralization of inorganic salts or sol−gel materials. Polylysine has been studied in biomineralization and is capable of forming ordered

silica structures.[48] Euliss et al.[49] also studied the formation of calcium carbonate microspheres directed by doubly hydrophilic block copolypeptides containing oligolysine blocks. Our mesosized single-crystal lamellae with periodic functionality displayed on the surface provide a promising substrate for use in biomineralization and hybrid material self-assembly.

Acknowledgment. Funding was provided by the NSF Career Award (DMR-0348147), UCSB/NSF-NIRT (DMR-0080034), and DuPont Young Faculty Award. We also thank the W. M. Keck College of Engineering electron microscopy lab at the University of Delaware. Synchrotron beamtime was provided by the National Synchrotron Light Source, Brookhaven National Laboratory, which is supported by the U.S. Department of Energy, Division of Materials Sciences and Division of Chemical Sciences, under Contract DE-AC02-98CH-10886.

References and Notes

(1) Winfree, E.; Liu, F. R.; Wenzler, L. A.; Seeman, N. C. *Nature (London)* **1998**, *394*, 539−544.
(2) Le, J. D.; Pinto, Y.; Seeman, N. C.; Musier-Forsyth, K.; Taton, T. A.; Kiehl, R. A. *Nano Lett.* **2004**, *4*, 2343−2347.
(3) Misner, M. J.; Skaff, H.; Emrick, T.; Russell, T. P. *Adv. Mater.* **2003**, *15*, 221−224.
(4) Sone, E. D.; Zubarev, E. R.; Stupp, S. I. *Angew. Chem., Int. Ed.* **2002**, *41*, 1705−1709.
(5) Fischer, E. W. *Naturforsch* **1957**, *12*, 753−754.
(6) Keller, A. *Philos. Mag.* **1957**, *2*, 1171−1175.
(7) Till, P. H. *J. Polym. Sci.* **1957**, *24*, 301−306.
(8) Geil, P. H. *Polymer Single Crystals*; John Wiley & Sons: New York, 1963.
(9) Krejchi, M. T.; Atkins, E. D. T.; Waddon, A. J.; Fournier, M. J.; Mason, T. L.; Tirrell, D. A. *Science* **1994**, *265*, 1427−1432.
(10) Krejchi, M. T.; Cooper, S. J.; Deguchi, Y.; Atkins, E. D. T.; Fournier, M. J.; Mason, T. L.; Tirrell, D. A. *Macromolecules* **1997**, *30*, 5012−5024.
(11) Spegt, P. *Makromol. Chem.* **1970**, *140*, 167.
(12) Cheng, S. Z. D.; Zhang, A. Q.; Barley, J. S.; Chen, J. H.; Habenschuss, A.; Zschack, P. R. *Macromolecules* **1991**, *24*, 3937−3944.
(13) Kim, I.; Krimm, S. *Macromolecules* **1996**, *29*, 7186−7192.
(14) Buckley, C. P.; Kovacs, A. J. In *Structure of Crystalline Polymers*; Hall, I. H., Ed.; Elsevier Applied Science Publishers: Amsterdam, 1984; pp 261−307.
(15) Ungar, G.; Stejny, J.; Keller, A.; Bidd, I.; Whiting, M. C. *Science* **1985**, *229*, 386−389.
(16) Ungar, G.; Zeng, K. B. *Chem. Rev.* **2001**, *101*, 4157−4188.
(17) Padden, F. J.; Keith, H. D. *J. Appl. Phys.* **1965**, *36*, 2987−2995.
(18) Padden, F. J.; Keith, H. D.; Giannoni, G. *Biopolymers* **1969**, *7*, 793−804.
(19) Keith, H. D.; Giannoni, G.; Padden, F. J. *Biopolymers* **1969**, *7*, 775−792.
(20) Keith, H. D.; Padden, F. J.; Giannoni, G. *J. Mol. Biol.* **1969**, *43*, 423−438.
(21) Lotz, B. *J. Mol. Biol.* **1974**, *87*, 169−180.
(22) Colonnac, F.; Premilat, S.; Lotz, B. *J. Mol. Biol.* **1974**, *87*, 181−191.
(23) Andries, J. C.; Walton, A. G. *Biopolymers* **1969**, *8*, 465−474.
(24) Price, C.; Harris, P. A.; Holton, T. J.; Stubbersfield, R. *Polymer* **1975**, *16*, 69−71.
(25) Kumamaru, F.; Kajiyama, T.; Takayanagi, M. *J. Macromol. Sci.* **1978**, *B15*, 87−105.
(26) Itoh, K.; Foxman, B. M.; Fasman, G. D. *Biopolymers* **1976**, *15*, 419−455.
(27) Zimmerman, S. S.; Clark, J. C.; Mandelkern, L. *Biopolymers* **1975**, *14*, 585−596.
(28) Rybnikar, F.; Geil, P. H. *Makromol. Chem.* **1972**, *158*, 39.
(29) Carr, S. H.; Walton, A. G.; Baer, E. *Biopolymers* **1968**, *6*, 469−477.
(30) Lotz, B.; Keith, H. D. *J. Mol. Biol.* **1971**, *61*, 201.
(31) Lotz, B.; Keith, H. D. *J. Mol. Biol.* **1971**, *61*, 195.
(32) Tajima, Y.; Anderson, M.; Geil, P. H. *Int. J. Biol. Macromol.* **1979**, *1*, 98−106.
(33) Tajima, Y.; Anderson, J. M.; Geil, P. H. *Int. J. Biol. Macromol.* **1980**, *2*, 186−192.
(34) Deming, T. J. *Macromolecules* **1999**, *32*, 4500−4502.
(35) Deming, T. J. *Nature (London)* **1997**, *390*, 386−389.
(36) Shmueli, U.; Traub, W. *J. Mol. Biol.* **1965**, *12*, 205−214.
(37) Suwalsky, M.; Llanos, A. *Biopolymers* **1977**, *16*, 403−413.
(38) Wright, D. A.; Marsh, R. E. *Acta Crystallogr.* **1962**, *15*, 54−64.
(39) Kovacs, A. J.; Straupe, C. *J. Cryst. Growth* **1980**, *48*, 210−226.
(40) Wunderlich, B.; Arakawa, T. *J. Polym. Sci., Part A* **1964**, *2*, 3697.
(41) Yamamoto, T.; Miyaji, H.; Asai, K. *Jpn. J. Appl. Phys.* **1977**, *16*, 1891−1898.
(42) Bassett, D. C.; Block, S.; Piermari, Gj. *J. Appl. Phys.* **1974**, *45*, 4146−4150.
(43) Bassett, D. C.; Turner, B. *Philos. Mag.* **1974**, *29*, 285−307.
(44) Hikosaka, M.; Amano, K.; Rastogi, S.; Keller, A. *Macromolecules* **1997**, *30*, 2067−2074.
(45) Hikosaka, M.; Sakurai, K.; Ohigashi, H.; Koizumi, T. Jpn. *J. Appl. Phys.* **1993**, *32*, 2029−2036.
(46) Hikosaka, M.; Rastogi, S.; Keller, A.; Kawabata, H. *J. Macromol. Sci.* **1992**, *B31*, 87−131.
(47) Fuhrhop, J. H.; Krull, M.; Buldt, G. *Angew. Chem., Int. Ed. Engl.* **1987**, *26*, 699−700.
(48) Patwardhan, S. V.; Clarson, S. J. *Mater. Sci. Eng., C* **2003**, *23*, 495−499.
(49) Euliss, L. E.; Trnka, T. M.; Deming, T. J.; Stucky, G. D. *Chem. Commun.* **2004**, 1736−1737.

MA050776Q